

# A New Phase of Oriented Mesoporous Silicate Thin Films

Sarah H. Tolbert,<sup>†,⊥</sup> Tilman E. Schäffer,<sup>‡</sup> Jianglin Feng,<sup>§</sup> Paul K. Hansma,<sup>‡</sup> and Galen D. Stucky<sup>\*,†</sup>

Department of Chemistry, University of California, Santa Barbara, California 93106-9510;  
Department of Physics, University of California, Santa Barbara, California 93106; and  
Center for Quantized Electronic Structures, University of California,  
Santa Barbara, California 93106

Received August 29, 1996. Revised Manuscript Received May 15, 1997<sup>Ⓢ</sup>

The syntheses and characterization of silicate/surfactant thin films with the structure  $P6_3/mmc$  is presented. The films are synthesized using a novel double-headed quaternary amine surfactant and can be grown either on mica or at the air–water interface. Films are shown to be crystalline and oriented with the  $c$ -axis perpendicular to the plane of the film. The films can be calcined to remove the surfactant and produce a mesoporous silicate material. Evidence is presented that suggests that films nucleate on hexagonally close packed surfactant micelles.

## Introduction

The recent discovery of mesoporous silicates<sup>1</sup> formed by the cooperative self-assembly<sup>2</sup> of silicates and surfactants has opened up a new range of possibilities for separation and catalysis involving large molecules. These materials, which can be made with pore diameters ranging from 15 Å to over 100 Å provide porosity on a unique new length scale and offer hope for processing of molecules too large to fit in the pores of traditional zeolites.<sup>1,3</sup>

For many applications of mesoporous silicates, thin films, both supported and unsupported, would be an ideal morphology. These applications include, but are not limited to, size- and shape-selective separation membranes<sup>4</sup> and size- and shape-selective chemical sensors based on piezoelectric mass balances such as the surface acoustic wave (SAW) device or the quartz crystal microbalance.<sup>4</sup> To this end, researchers at the University of Toronto<sup>5,6</sup> and at Princeton University<sup>7</sup> have recently produced thin films of the two-dimensional hexagonal array silicate, MCM-41. These films can be grown on both mica surfaces<sup>5</sup> and graphite surfaces<sup>7</sup> and as free-standing films at the air–water

interface.<sup>6</sup> In addition, the films can be calcined to remove the surfactant and produce a true mesoporous material. Unfortunately, in all morphologies, the pore structure runs rigorously parallel to the film and thus does not allow easy transport in to or through the film.

To address this problem, we present here the synthesis and characterization of mesoporous silicate films, both on mica and unsupported, in the structure SBA-2.<sup>8</sup> These films have space group  $P6_3/mmc$  and can be considered to consist of hexagonally close-packed spheres, ellipsoids, or interconnected ellipsoids. Although the details of the pore structure are not yet well understood, BET surface areas on the order of 900 m<sup>2</sup>/g have been observed. The films are oriented with the  $c$ -axis normal to the plane of the film. As an undulating pore system with a component parallel to the  $c$ -axis is likely for these materials, they should provide a pore morphology which allows transport normal to the silicate film.

These films are synthesized using a novel two-headed (or gemini) quaternary ammonium surfactant.<sup>3,9</sup> In this paper, we describe the use of 18-3-1, a surfactant consisting of an 18-carbon aliphatic chain attached to a dimethyl quaternary ammonium. This charged headgroup is then connected via a 3-carbon linker to a second trimethyl quaternary ammonium. The large size and high charge of the surfactant headgroup stabilize structures with very high interfacial curvature such as the  $P6_3/mmc$  phase described above. Other related configurations such as 16-3-1, 20-3-1, or 18-6-1 can be used as well and are observed to assemble with the same  $c$ -axis orientation.

The highly oriented nature of these films is achieved by utilizing acid synthesis conditions.<sup>10,11</sup> In this prepa-

<sup>†</sup> Department of Chemistry.

<sup>‡</sup> Department of Physics.

<sup>§</sup> Center for Quantized Electronic Structures.

<sup>⊥</sup> Permanent address: Department of Chemistry & Biochemistry, University of California, Los Angeles, CA 90095-1569.

<sup>Ⓢ</sup> Abstract published in *Advance ACS Abstracts*, July 1, 1997.

(1) Kresge, C. T.; Leonowicz, M. E.; Roth, W. J.; Vartuli, J. C.; Beck, J. S. *Nature* **1992**, *359*, 710. Beck, J. S.; Vartuli, J. C.; Roth, W. J.; Leonowicz, M. E.; Kresge, C. T.; Schmitt, K. T.; Chu, C. T.-W.; Olson, D. H.; Sheppard, E. W.; McCullen, S. B.; Higgins, J. B.; Schlenker, J. L. *J. Am. Chem. Soc.* **1992**, *114*, 10834.

(2) Firouzi, A.; Kumar, D.; Bull, L. M.; Besier, T.; Sieger, P.; Huo, Q.; Walker, S. A.; Zasadzinski, J. A.; Glinka, C.; Nicol, J.; Margolese, D.; Stucky, G. D.; Chmelka, B. F. *Science* **1995**, *267*, 1138.

(3) Huo, Q.; Margolese, D. I.; Stucky, G. D. *Chem. Mater.* **1996**, *8*, 1147.

(4) Bein, T. *Chem. Mater.* **1996**, *8*, 1636.

(5) Yang, H.; Kuperman, A.; Coombs, N.; Mamiche-Afara, S.; Ozin, G. A. *Nature* **1996**, *379*, 703.

(6) Yang, H.; Coombs, N.; Sakolov, I.; Ozin, G. A. *Nature* **1996**, *381*, 589.

(7) Aksay, I. A.; Trau, M.; Manne, S.; Honma, I.; Yao, N.; Zhou, L.; Fenter, P.; Eisenberger, P. M.; Gruner, S. M. *Science* **1996**, *273*, 892.

(8) Huo, Q.; Leon, R.; Petroff, P. M.; Stucky, G. D. *Science* **1995**, *268*, 1324.

(9) Zana, R.; Benraou, M.; Rueff, R. *Langmuir* **1991**, *7*, 1072. Zana, R.; Talmon, Y. *Nature* **1993**, *362*, 228.

(10) Huo, Q.; Margolese, D. I.; Ciesla, U.; Feng, P.; Gier, T. E.; Sieger, P.; Leon, R.; Petroff, P. M.; Schüth, F.; Stucky, G. D. *Nature* **1994**, *368*, 317.

(11) Huo, Q.; Margolese, D. I.; Ciesla, U.; Demuth, D. G.; Feng, P.; Gier, T. E.; Sieger, P.; Firouzi, A.; Chmelka, B. F.; Schüth, F.; Stucky, G. D. *Chem. Mater.* **1994**, *6*, 1179.

ration, both the surfactant and the silicate species are positively charged. Their interaction is mediated by a halogen ion (in this case  $\text{Cl}^-$ ) which provides the stabilization needed for self-assembly. This contrasts sharply to the more common basic synthesis conditions where negatively charged silicate species form tight ion pairs with positively charged surfactants. Because of the weak interaction between surfactant and silicate, the stabilization that results in surfactant self-assembly at interfaces can be energetically significant when compared to the stabilization resulting from mesophase assembly. Thus, surfactant surface assemblies likely remain intact in the presence of acidic silicate species and can act as nucleation sites for highly oriented thin films of silicate/surfactant composites. This novel synthesis approach was also utilized for thin film MCM-41 preparations on mica,<sup>5</sup> graphite,<sup>7</sup> and at the air–water interface,<sup>6</sup> for silica condensation in the presence of liquid-crystal phases,<sup>12</sup> and for the synthesis of hollow mesoporous spheres or fibers.<sup>13</sup>

### Experimental Section

Silicate/surfactant films with space group  $P6_3/mmc$  were synthesized from an acidic HCl solution. Films on mica were grown according to ref 5, starting with a reaction mixture containing water:HCl:18-3-1:TEOS (tetraethyl orthosilicate) in molar ratios of 100:7.4–7.5:0.09–0.10:0.18–0.23. Mica samples were freshly cleaved and held upside down in solution to prevent bulk precipitate from sticking to the surface. Films were grown at 80 °C under hydrothermal conditions for times ranging from 12 h to 1 week; films were washed with water after removal from the growth medium. Unsupported films were grown at the air–water interface according to ref 6. Reaction mixtures contained water:HCl:18-3-1:TEOS in molar ratios of 100:7.4:0.09–0.11:0.18–0.34. Films were grown at room temperature or at 80 °C for times ranging from 12 h to 1 week. Before collecting the films, water was added slowly to the film growth medium to separate the surface film from the underlying bulk precipitate. Films were collected onto glass or mica slides and onto uncoated TEM grids. Films were allowed to dry without rinsing.

Both air–water interface and mica films were calcined to remove the surfactant. Films were heated from room temperature to 500 °C under nitrogen over the course of 8 h. Films were then allowed to sit at 500 °C under nitrogen for 6 h. The gas was changed to oxygen and the films were left at 500 °C for another 6 h. This was followed by a 4 h return to room temperature, also under oxygen. Air–water interface films on Ni TEM grids were calcined to only 400 °C to prevent extreme warping of the TEM grids. This slow calcination procedure was employed in an effort to minimize film cracking due to thermal stress. The bulk precipitates of these films were calcined by slowly heating under nitrogen to 350 °C, followed by continued heating under oxygen to 500 °C and a 6 h hold under oxygen at 500 °C. Bulk samples were analyzed for porosity using nitrogen absorption isotherms recorded on a Micromeritics ASAP 2000 porosimeter. Surface area was determined by the BET (Brunauer–Emmett–Teller) method; pore volumes were determined from a single point measurement at  $P/P_0 = 0.9837$ . Pore-size distribution was determined by the BJH (Barrett–Joyner–Halenda) method.

X-ray diffraction data were obtained using a Scintag Pad X diffractometer equipped with a liquid nitrogen cooled germanium solid-state detector and  $\text{Cu K}\alpha$  radiation. Integration times varied from 2 to 4 s/point. AFM data of a 7 mM

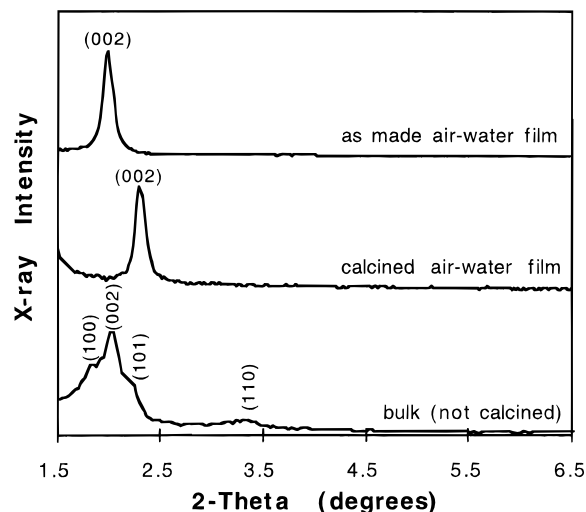


**Figure 1.** X-ray diffraction of silicate/surfactant composite films grown at the air–water interface. Films are grown with the gemini surfactant 18-3-1 under acidic conditions. Top: as-made films show the intense (002) diffraction peak of the  $P6_3/mmc$  phase, indicating that the films are  $c$ -axis oriented. Middle: the same films as shown above after calcination to remove the surfactant. Some decrease in the lattice constant is observed. Bottom: an uncalcined bulk sample is shown for comparison.

surfactant solution on mica were collected on a Digital Instruments Nanoscope III<sup>14</sup> equipped with a fluid cell. A silicon nitride cantilever (Digital Instruments) was scanned over the surface in contact mode at 8 lines/s. Imaging forces were minimized and estimated to be on the order of 1 nN. SEM images of mica-supported silicate/surfactant films were obtained with a JEOL JSM-5300LV scanning electron microscope. Samples were attached to the stub with conducting carbon tape and sputtered with gold prior to imaging. SEM images on air–water films (with the exception of Figure 6b) were collected on uncoated samples using a JEOL JSM-6300F instrument equipped with a cold cathode field emission source. A beam energy of 3 keV was used in combination with an electron probe current of  $3 \times 10^{-12}$  A to reduce sample charging. Figure 6b was obtained in a configuration similar to that used for the mica-supported films.

### Results

X-ray diffraction data obtained on silicate/surfactant films grown at the air–water interface are shown in Figure 1. These films were grown at room temperature and lifted onto either mica or glass slides with no apparent difference. The top trace is for an uncalcined film and shows only one intense diffraction peak.<sup>15</sup> This peak agrees well with the (002) diffraction peak observed in bulk silicate/surfactant composites with the structure  $P6_3/mmc$  (bottom trace). From these data, we can conclude (1) that the films are crystalline and (2) that the films are oriented with the  $c$ -axis perpendicular to the plane of the film. After calcination (middle trace), a 16% decrease in the lattice constant is observed. This change is consistent with shrinkage observed in bulk silicate/surfactant composites upon calcination. Film integrity is preserved upon calcination.

The orientation of the air–water films is confirmed by TEM analysis of calcined films grown at 80 °C

(12) Attard, G. S.; Glyde, J. C.; Göltner, C. G. *Nature* **1995**, *378*, 366.

(13) Schacht, S.; Huo, Q.; Voigt-Martin, I. G.; Stucky, G. D.; Schüth, F. *Science* **1996**, *273*, 768. Huo, Q. S.; Zhao, O.; Feng, J. L.; Weston, K.; Buratto, S.; Stucky, G. D.; Schacht, S.; Schüth, F. *Adv. Mater.*, in press.

(14) Digital Instruments, Santa Barbara, CA.

(15) A very faint (004) diffraction peak can be observed in some samples. This peak is too weak to be seen in the bulk material, however.

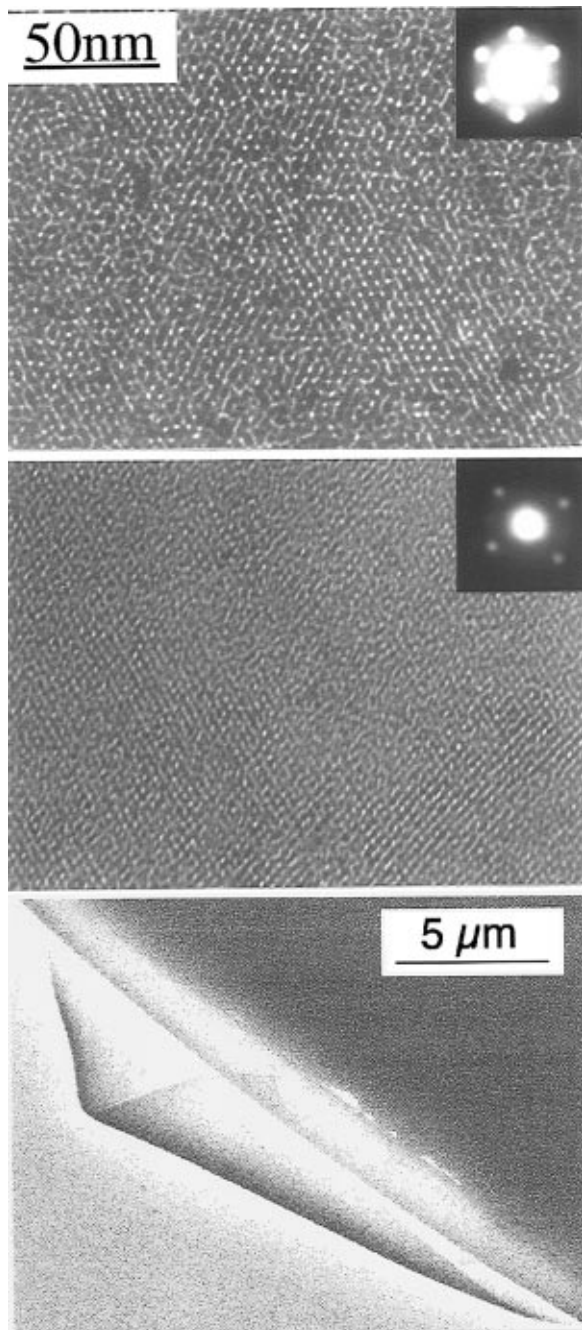


**Figure 2.** Top: TEM image and electron diffraction pattern of the major orientation observed in calcined silicate films with the structure  $P6_3/mmc$  grown at 80 °C. The data show highly crystalline films with the  $c$ -axis oriented perpendicular to the plane of the film ([0001] zone axis). Middle: TEM image of the minor orientation observed in calcined silicate films with the structure  $P6_3/mmc$  grown at 80 °C ([01 $\bar{1}$ 1] zone axis) [same scale as the top image]. This orientation is observed in thin sections of the film near edges. The observation of [01 $\bar{1}$ 1] and [11 $\bar{2}$ 3] oriented material (the latter obtained by tilting and is not shown here) confirms the  $P6_3/mmc$  structure of the films. Bottom: Low-resolution TEM image of a  $P6_3/mmc$  silicate film showing that films are flexible and have good long-range structural integrity. Scale bars are shown on the images. The scale for the top and middle images is the same.

(Figure 2). Uncalcined films and calcined films grown at room temperature produced somewhat lower quality and less well oriented images. Figure 2 (top) shows a TEM image of the major orientation observed in these films. The clear hexagonal array observed in the image and the clean hexagonal electron diffraction pattern

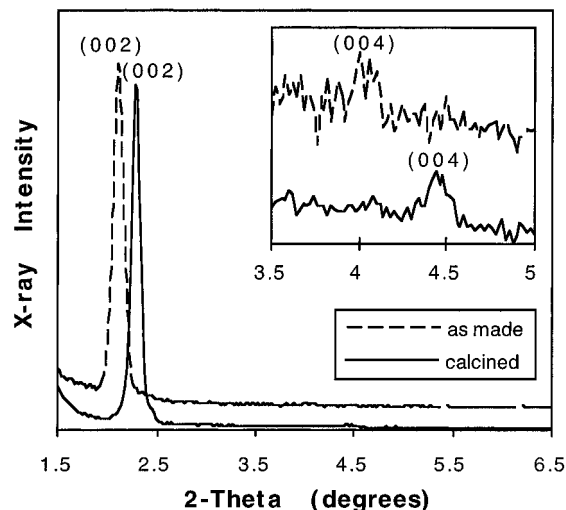


**Figure 3.** X-ray diffraction of silicate/surfactant composite films grown on mica surfaces. The traces correspond to calcined (solid line) and uncalcined (dashed line) samples. Patterns are offset vertically for clarity. The presence of only the (002) and (004) diffraction peaks in each pattern demonstrates that the films are crystalline and oriented on the mica surface. An 8% lattice contraction is observed upon calcination.

(inset) confirm the  $c$ -axis orientation of the films.<sup>8</sup> This type of image is observed in the areas of the film with normal thickness. A secondary orientation is also observed in the thin sections of the films, particularly at the edges of film pieces. Shown in Figure 2 (middle), this image and electron diffraction pattern can be assigned to the [01 $\bar{1}$ 1] zone axis of the  $P6_3/mmc$  phase.<sup>8</sup> Multiple explanations for this structure in the thin sections of the film can be hypothesized. It is possible that these domains result from shearing of the major orientation when films are broken and put onto TEM grids. Reorientation of the film edges upon calcination is also a possibility. Alternatively, sections of the film which happen to nucleate with an [01 $\bar{1}$ 1] orientation could simply show slower growth, compared to the [0001] major orientation. In agreement with these TEM results, in some cases small (0111) X-ray diffraction peaks with intensity less than 1:100 compared to the (002) diffraction peak are observed in these films.<sup>16</sup> The observation of indexable [0001] and [01 $\bar{1}$ 1] TEM images further corroborates the assignment of  $P6_3/mmc$  for the structure of these films.

High-resolution TEM also shows that the films are crystalline and homogeneous over large areas. Furthermore, low-resolution TEM images (Figure 2, bottom) can be used to illustrate both the flexibility and long-range structural integrity of these materials. Film pieces similar to this in the 3–10 mm length scale can be readily produced.

Figure 3 shows X-ray diffraction patterns for silicate/surfactant films grown epitaxially on freshly cleaved mica. Uncalcined and calcined films are shown with dashed and solid lines, respectively. The patterns are offset vertically for clarity. Only (002) and (004) diffraction peaks are observed in both patterns. This fact, combined with the high intensity and narrow widths of the diffraction peaks, confirms the very oriented, very

(16) The (0111) diffraction peak in the four index hexagonal notation is equivalent to the (101) diffraction peak in three hexagonal index notation shown in Figure 1.

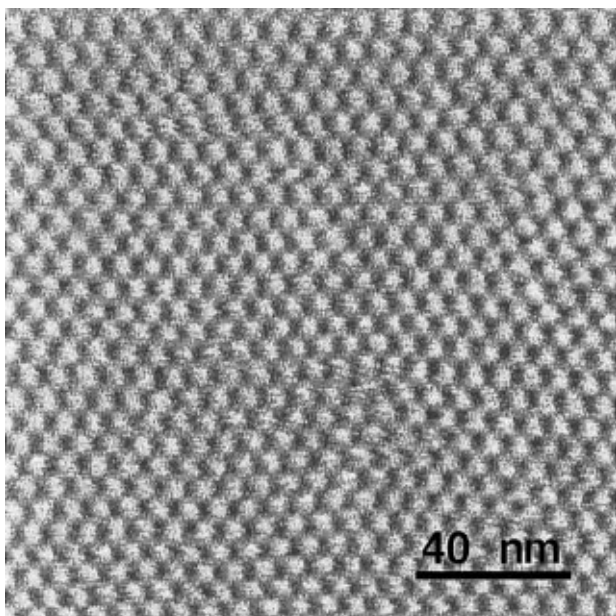


**Figure 4.** AFM image of pure 18-3-1 surfactant on a freshly cleaved mica surface. Hexagonally close-packed micelles can be clearly seen. These structures likely serve as a nucleation site for the silicate/surfactant films described above. Scale bar = 40 nm.

crystalline nature of these films. Because these films were grown at 80 °C, less shrinkage is observed upon calcination, compared to the room-temperature air-water films described above. A lattice contraction of only 8% is observed in the  $d$  spacings upon calcination. This value is consistent with bulk samples grown under these conditions. Unlike the air-water interface films, however, the film shrinkage results in some film cracking upon calcination because these films are bonded to the mica substrate. When calcined under appropriate conditions, homogeneous film domains on the order of 100  $\mu\text{m}$  are observed. Supported, cracked films of this type could find application in areas such as piezoelectric-based chemical sensors which do not require gastight films to function.

## Discussion

**(1) Nucleation and Growth of Films.** The process by which tightly bonded silicate/surfactant films grow on mica surfaces can be understood by first considering the bonding of pure surfactants to mica surfaces. Figure 4 shows an AFM image of the two-headed surfactant 18-3-1 in the presence of a freshly cleaved mica surface.<sup>17</sup> A hexagonal array of spheres can be clearly seen. This structure maximizes the curvature of the surfactant phase, allowing highly charged headgroups to be as far from each other as possible. At the same time, it allows for significant bonding between the positively charged surfactant headgroups and the negatively charged mica surface. In the presence of solution-phase silicate species at acid pH, these structures are also observed.<sup>18</sup>

A hexagonal array of surfactant spheres corresponds to an  $a$ - $b$  plane of the  $P6_3/mmc$  phase and thus serves as an ideal nucleation site for  $c$ -axis oriented surfactant/

silicate composites. Because the synthesis conditions utilize strong acid as opposed to strong base, it appears that the bonding between silicates and surfactants is not strong enough to disrupt this surface surfactant layer. We thus propose that surface-bound micelles act as a template to nucleate growth of the  $P6_3/mmc$  phase.<sup>17,19</sup> This nucleation is likely followed by cooperative addition of further silicate and surfactant species.

We note that only three ordered two-dimensional structures are known for surfactants self-assembled at interfaces.<sup>17</sup> These are layers, rods,<sup>19</sup> and spheres (in both monolayer and bilayer or micelle and hemimicelle form, depending on the interface polarity). Consideration of the known silicate/surfactant species that could be nucleated off these self-assembled surfactant structures produces lamellar,  $p6m$  (2-D) hexagonal, and a supercage structure such as  $P6_3/mmc$  for the material nucleated off layers, rods, and spheres, respectively. Of these structures, only the  $P6_3/mmc$  or a related cubic supercage material<sup>20</sup> has the potential for a pore system with a component perpendicular to the plane of the film.

SEM can also be used to learn about the growth of these films. Unlike the AFM image presented above, the length scales of SEM images are far from the molecular regime. Insight into the growth process can be gained, however, by examining the overall film morphology. Figure 5a,b shows SEM images of silicate/surfactant films grown on mica with the gemini surfactant 18-3-1 at 80 °C. Figure 5b shows a film that was grown for only 12 h. The film is seen to consist of interconnected circular or rounded hexagonal domains. This morphology is consistent with the expected growth pattern for  $c$ -axis oriented  $P6_3/mmc$  phase material. The films should have six symmetry-related growth directions which should produce hexagonal or nearly round islands.

For comparison, an image of a film grown for short times with the single-headed surfactant hexadecyl trimethylammonium bromide (CTAB) is shown in Figure 5c.<sup>5</sup> The CTAB film consists of hexagonally packed columns (MCM-41) with the  $c$ -axis oriented in the plane of the film.<sup>5</sup> The film structure in Figure 5c is clearly quite different from that observed in Figure 5b. Consistent with a uniaxial in-plane easy growth direction, the film consists of stripes of silicate material with an aspect ratio on the order of 10:1. From these data, we can conclude that overall film morphology is strongly affected by film structure and can thus be used to gain insight into the orientation and growth processes in these materials.

Figure 5a shows a  $P6_3/mmc$  phase film that was grown for a significantly longer period of time (3 days). By this time, the film is continuous and is seen to consist of overlapping circular or hexagonal domains. The domain size is not, however, significantly bigger than those observed in Figure 5b. It is possible that strain

(19) Manne, S.; Cleveland, J. P.; Gaub, H. E.; Stucky, G. D.; Hansma, P. K. *Langmuir* **1994**, *10*, 4409. Manne, S.; Gaub, H. E. *Science* **1995**, *270*, 1480.

(20) Several supercage phases are known in the surfactant literature (Luzzati, V., Delacroix, H. Gulik, A. *J. Phys. II France*, **1996**, *6*, 405). Of these, only the  $Pm3n$  phase<sup>10</sup> has been reported as a silicate/surfactant composite, and this phase does not have the correct symmetry to nucleate on a hexagonally close packed monolayer of spherical micelles. If it could be made as a silicate/surfactant composite, a cubic phase such as the  $Fm3m$  could nucleate from a surfactant layer like that shown in Figure 4.

(17) Manne, S.; Schäffer, T. E.; Huo, Q.; Hansma, P. K.; Morse, D. E.; Aksay, I. A.; Stucky, G. D., submitted.

(18) Tolbert, S. H.; Schäffer, T. E., unpublished results.

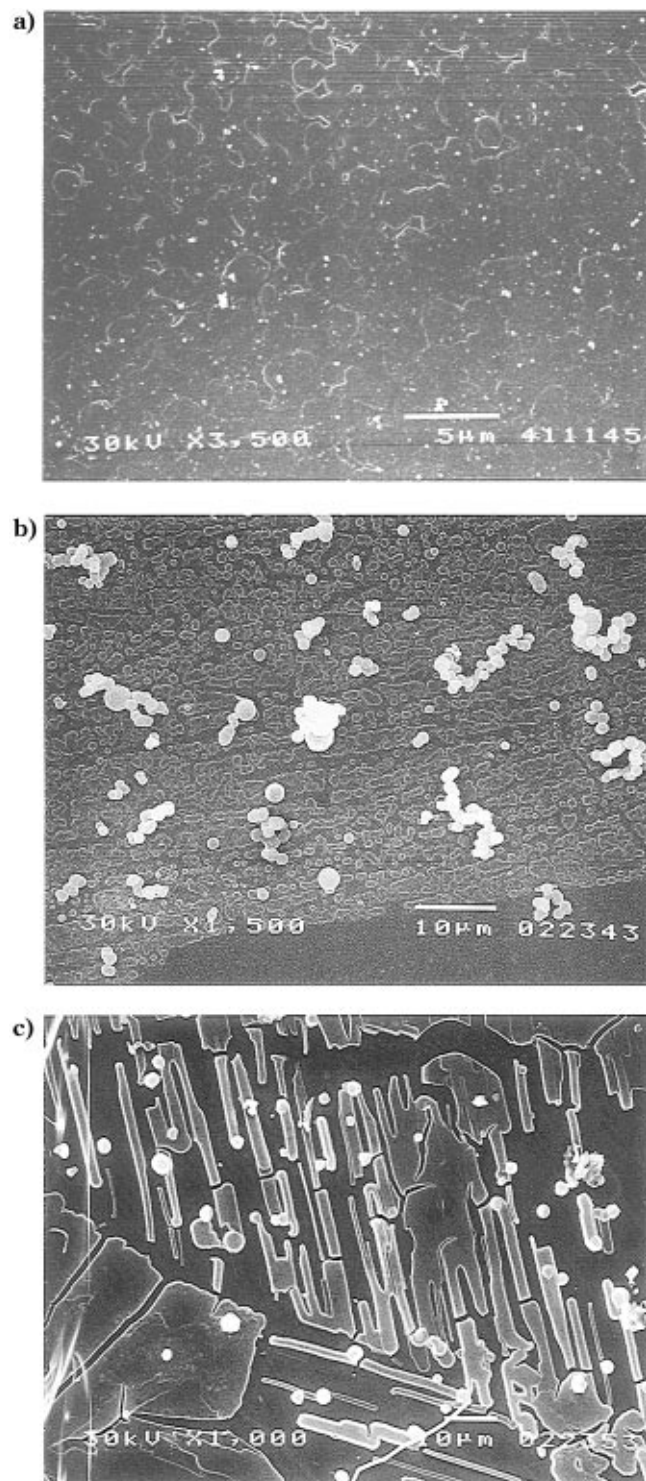


**Figure 5.** SEM images of silicate/surfactant films grown at 80 °C on freshly cleaved mica. The solid white spheres in parts (b) and (c) are pieces of bulk composite which settled on the films during growth. These spheres can be avoided by holding the films upside down in solution during growth [see part (a)]. (a)  $P6_3/mmc$  film grown for 3 days shows homogeneous coverage, consisting of overlapping circular or hexagonal domains. (b)  $P6_3/mmc$  film grown for only 12 h, showing spotty domains. The circular/hexagonal symmetry of the domains reflects the overall structure of the films. (c) A  $p6m$  (CTAB) film is included for comparison. In this case, the  $c$ -axis of the  $p6m$  phase lies in the plane of the film and produces a different overall morphology.

produces a limiting domain size in these materials, and thus further growth changes only the domain density and not the domain size.

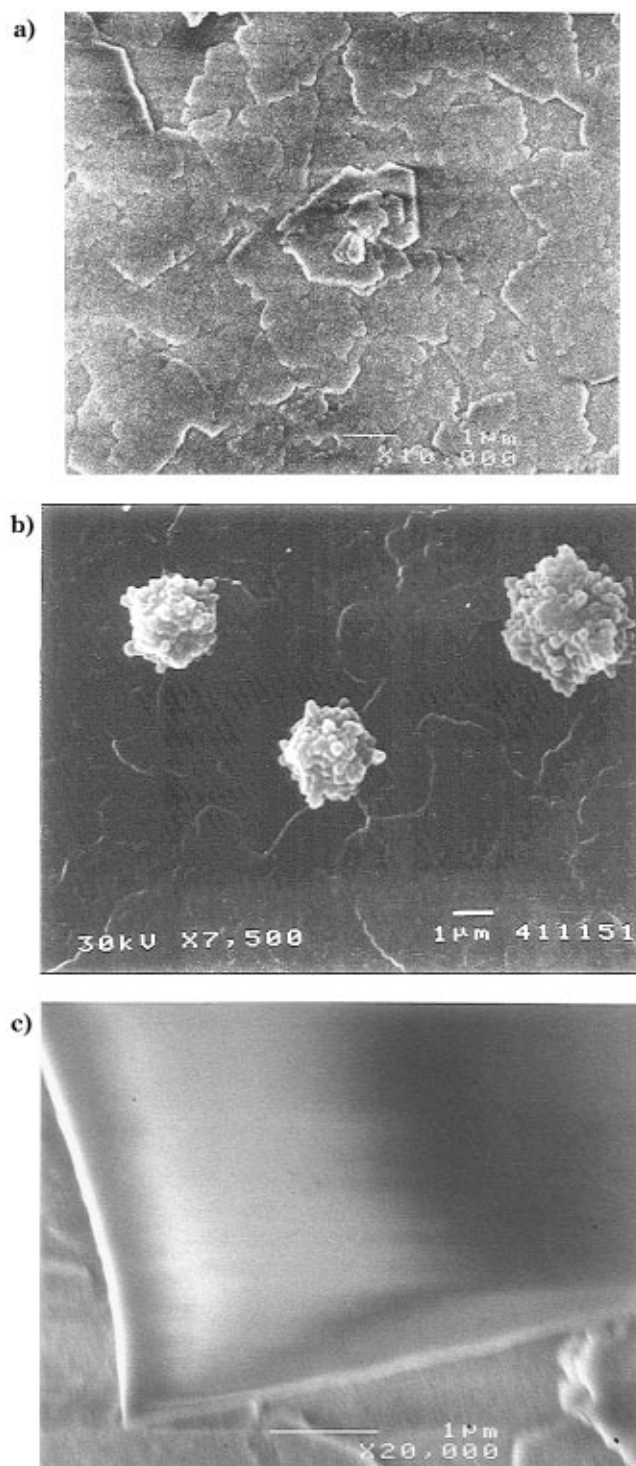


**Figure 6.** SEM images of  $P6_3/mmc$  silicate/surfactant films grown at room temperature at the air-water interface. The water side of the film is shown in parts (a) and (b). Part (a) shows overlapping domains similar to those observed in Figure 5. Part (b) shows dendritic structures which can be found on parts of the film. The structures appear hexagonal and thus confirm the orientation of the films. Part (c) shows the air surface of the films which are completely flat on the SEM length scale. A corner is included to prove that the image is in focus.

SEM images of films grown at the air-water interface at room temperature are shown in Figure 6. Because these films are not supported on substrates, it is possible to image both the air and the water surface of the film. Figure 6a shows an image of a typical water surface of an air-water film. The image looks very similar to the



mica film shown in Figure 5a, as might be expected. After nucleation at either the air–water interface or a mica surface, growth into solution should proceed by similar mechanisms in both cases. The largest structures observed in this image are approximately 1–2  $\mu\text{m}$ , with smaller undulations on the order of 100–200 nm. These smaller structures agree well with the domains observed in TEM experiments and so can be assigned to the actual domain size of the material.

One difference between air–water interface and mica films is seen in Figure 6b. In some cases, the water side of air–water films show dendritic structures that have clearly nucleated off the films and grown down into solution. These structures could result from the lower growth temperature in this air–water film (room temperature), compared to the mica films shown in Figure 5 (80 °C). Alternatively, they could represent an intrinsic difference in growth form between the two types of films due to different internal strain or different types of defects. The hexagonal symmetry of the dendrites confirms the orientation of the air–water films. The presence of these structures proves that nucleation sites are an important requirement for the growth of oriented silicate/surfactant composites.

In sharp contrast with Figure 6a,b, Figure 6c shows an SEM image of the air surface of an air–water film. The edge of a broken piece of film is included to prove that the image is in focus. The air surfaces are completely flat on the length scale of the SEM. This result is consistent with data presented earlier for the air surface of CTAB air–water films<sup>6</sup> and strongly suggests that films nucleate on surfactants that aggregate in a monolayer or multilayer type structure at the air–water interface. Given the structure of this surfactant, hemimicelles are a possibility for the interface aggregate which nucleate  $P6_3/mmc$  structure films.<sup>19</sup>

**(2) Porosity.** A key issue for the usefulness of these films, in comparison to the CTAB films which have been reported earlier,<sup>5–7</sup> lies in the film porosity normal to the plane. The CTAB films have a pore structure that runs parallel to the plane of the film and thus limits the use of the films in applications such as catalysis, separation, or chemical sensing. While the details of the pore structure in the films presented above are not yet known, geometrically it is reasonable that the pores have a component perpendicular to the plane of these films. The  $P6_3/mmc$  phase with an ideal  $c/a$  ratio is the hexagonal close-packed structure (hcp). In the case of pure surfactants, this structure is thought to consist of hexagonally close-packed spherical or polygonal micelles.<sup>21</sup> For calcined bulk  $P6_3/mmc$  silicate/surfactant composites made with 18-3-1 surfactant, however, nitrogen absorption isotherms show a surface area of 885  $\text{m}^2/\text{g}$  (BET method) and a pore volume of 0.62  $\text{cm}^3/\text{g}$  (single-point method). The data also exhibit no hysteresis in the isotherms and a fairly narrow pore size distribution (BJH method). These data indicate the

presence of a well-defined pore structure in the material.

Since the diffraction pattern in these materials is unchanged upon calcination, the pore structure must reflect the symmetry of the lattice. Because of the very high symmetry of the hcp structure, a pore system which existed only in the  $a$ – $b$  plane would in fact have to be three interpenetrating pore systems resulting in six connections between each cavity and all of its planar nearest neighbors. It is unlikely that such a structure would be stable to calcination. More likely possibilities include an undulating pore system which runs parallel to the  $c$ -axis or has a component parallel to the  $c$ -axis, or a random pore structure (i.e., random connections between any quasi-spherical cavity and 2 or more of its 12 nearest neighbors). All of these possibilities would retain a component perpendicular to the plane of the film and would thus allow diffusion normal to the plane of the film.

## Conclusions

In this paper, we have presented data on the synthesis of silicate/surfactant films with the structure  $P6_3/mmc$  grown either at the air–water interface or on mica surfaces. X-ray diffraction and TEM were used to show that the films are stable to calcination, ordered, and oriented. Analyses of AFM and SEM images suggest that the films nucleate on micellar structures in an oriented fashion and then grow into the solution. Finally, consideration of BET results and symmetry constraints suggest that the pore structure in these materials likely has a component perpendicular to the plane of the film.

The production of silicate/surfactant composites in the form of porous thin films is a major step toward the use of these materials for purposes such as separation membranes or chemical sensors. The ease with which these films grow and the robust nature of the self-assembly process are added benefits to these types of materials. By utilizing novel surfactants with specific packing constraints, it should, in time, be possible to produce mesoporous films in a variety of structures with pore systems optimized for specific purposes.

**Acknowledgment.** The authors would like to thank Dr. Qisheng Huo for his advice and assistance in the synthesis of  $P6_3/mmc$  materials and the 18-3-1 surfactant. Funds for this work were provided by NSF Grant DMR 95-20971 (G.D.S. and S.H.T.), NSF postdoctoral research fellowship Grant CHE-9626523 awarded in 1996 (S.H.T.), and a University of California Training Grant (T.E.S.). J.F. acknowledges the support of QUEST, an NSF Science and Technology Center for Quantized Electronic Structures (Grant No. DMR 91-20007). This work made use of MRL Central Facilities supported by the NSF under Award DMR-9123048. We also thank Digital Instruments for AFM support.

CM9604540

(21) Clerc, M. *J. Phys. II France* **1996**, *6*, 961.